



Teleconnections between ENSO and North Atlantic in an ECHO-G simulation of the 1000–1990 period

Isabelle Gouirand,¹ Vincent Moron,^{1,2} and Eduardo Zorita³

Received 22 November 2006; revised 12 January 2007; accepted 6 February 2007; published 22 March 2007.

[1] The North Atlantic sea level pressure anomalies (SLPA) associated with El Niño Southern Oscillation (ENSO) have been analyzed in a quasi-millennial (1000–1990) simulation with the ECHO-G model. In November–December, the ENSO-related SLPA over the North Atlantic area are weak, while a realistic pattern already appears over the North Pacific and North America. In January–March, the SLPA over North Atlantic are stronger and realistic from the North Pacific to Europe: the Aleutian low is strengthened (weakened), SLPA are positive (negative) over the north-central and north-eastern parts of North America, and SLPA display a negative (positive) NAO-like pattern over North-Atlantic during warm (cold) ENSO events, as in observations. The results also confirm the existence of a strong inter-event SLPA associated with warm and cold ENSO events, especially over the North Atlantic, while the relationship is stationary at multidecadal timescales. It seems that neither the intensity nor geographical longitude of the equatorial Pacific sea surface temperature anomaly (SSTA) and intensity of tropical Atlantic SSTA, nor the volcanic forcing, simply introduced here as a decrease of the solar constant, significantly induce an inter-event variability, which seems, in this run, mostly of atmospheric origin. **Citation:** Gouirand, I., V. Moron, and E. Zorita (2007), Teleconnections between ENSO and North Atlantic in an ECHO-G simulation of the 1000–1990 period, *Geophys. Res. Lett.*, *34*, L06705, doi:10.1029/2006GL028852.

1. Introduction

[2] The relationships between El Niño Southern Oscillation (ENSO) and wintertime extratropical sea level pressure anomalies (SLPA) are well documented, especially over North Pacific and North America [Ropelewski and Halpert, 1987; Kumar and Hoerling, 1998; Pozo-Vazquez *et al.*, 2001; Lee *et al.*, 2002]. These studies indicate lower (higher) pressure than normal over the north-eastern part of the North Pacific and the south-eastern part of North America, and higher (lower) pressure than normal over the northern part of North America during the warm (cold) phase of ENSO. These anomalies are close to the Pacific-North-America or

Tropical North America patterns [i.e., Wallace and Gutzler, 1981; Mo and Livezey, 1986]. Over the North Atlantic, the SLPA associated with ENSO are weaker. The December–February SLPA during cold ENSO events resembles to a positive North Atlantic Oscillation (NAO)-like pattern, while those observed during the warm ENSO phase are weaker in absolute sense and close to a negative NAO-like pattern [May and Bengtsson, 1998; Pozo-Vazquez *et al.*, 2001]. Part of the weakness of the mean SLPA response in December–March stems from a seasonal modulation of the ENSO response between November and March [Huang *et al.*, 1998; Gouirand and Moron, 2003; Moron and Gouirand, 2003; Moron and Plaut, 2003]. A negative (positive) NAO-like pattern in the early winter (November–December) is followed by a positive (negative) one in the late winter (January–March) during cold (warm) ENSO phase. The linearity and stationarity of the North Atlantic SLPA relationship with ENSO have been discussed and a large inter-event variability, mainly during the warm phase of ENSO, has been established [Pozo-Vazquez *et al.*, 2001; Lee *et al.*, 2002; Moron and Gouirand, 2003].

[3] The analysis of ENSO teleconnection during the contemporaneous period is limited by the length of the observed record. One way to overcome this limitation is to use either climate reconstructions as Brönnimann *et al.* [2007] or long-term simulations from coupled ocean-atmosphere model. In this paper, a quasi-millennial ECHO-G (ECham Hope-G) run has been used to identify the ENSO teleconnection over North Atlantic and Europe on the period 1000–1990. The aim is to test whether the model driven only by variable solar radiation, a simple volcanism scheme and a realistic variation of greenhouse trace gases is able to reproduce the mean ENSO response over the North Atlantic domain and to identify possible origins of inter-event variability. Three different sources of inter-event variation will be considered here: (1) an external forcing (volcanism [i.e., Brönnimann *et al.*, 2007]), (2) an atmospheric forcing (intensity and polarity of North Pacific SLPA [i.e., Honda *et al.*, 2001]) and (3) an oceanic forcing (intensity and location of sea surface temperature anomalies (SSTA) over equatorial Pacific [i.e., Larkin and Harrison, 2005] and intensity of Tropical North Atlantic SSTA [i.e., Robertson *et al.*, 2000; Cassou and Terray, 2001]).

2. Data

[4] The AOGCM used in this paper is ECHO-G model [Legutke and Voss, 1999]. The atmospheric component is ECHAM4 [Roeckner *et al.*, 1996] and the ocean model is HOPE-G [Wolff *et al.*, 1997]. More details about this model are given by Min *et al.* [2005a, 2005b]. These authors showed that ECHO-G skillfully simulates the seasonal

¹Unité de Formation et de Recherche des Sciences Géographiques et de l'Aménagement et Centre Européen de Recherche et d'Enseignement des Géosciences de l'Environnement, UMR 6635 CNRS, University of Aix-Marseille, Aix-en-Provence, France.

²Also at International Research Institute for Climate and Society, Columbia University, New York, New York, USA.

³Gesellschaft für Kernenergieverwertung in Schiffbau und Schifffahrt, Geesthacht, Germany.

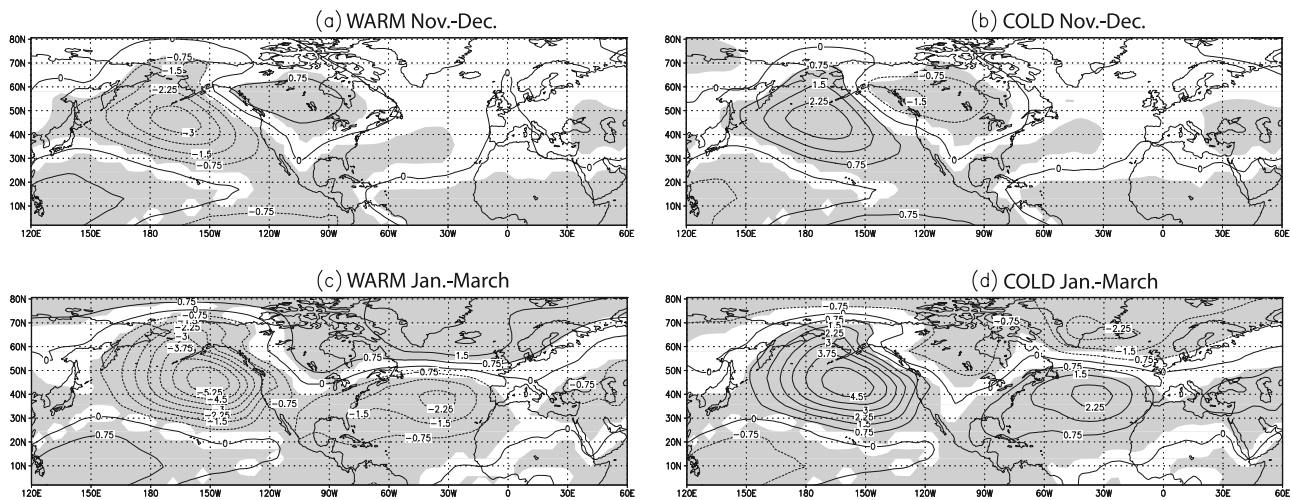


Figure 1. Mean sea level pressure anomaly (SLPA) (in hPa) in (a, b) November–December and (c, d) January–March during warm (Figures 1a and 1c) and cold (Figures 1b and 1d) ENSO events, respectively defined as Niño3 sea surface temperature anomalies (SSTA) $> 1\text{C}$ and $< -1\text{C}$. Positive (negative) SLPA are displayed as full (dashed) lines and shading indicates significant values at two-sided 10% significance level according to a Student’s t-test (the null hypothesis is that the difference between the cold and warm ENSO samples and the long-term mean is zero). SLPA and SSTA are high-pass filtered by removing all frequencies < 0.1 cycle-per-year before the analysis.

mean climatology and interannual variability of near surface temperature in the Tropical Pacific and sea level pressure in the North Atlantic. The seasonal cycle of the ENSO event is quite realistic but the frequency of warm and cold events is too high and too regular (one event every 2–3 years) compared to observations, and their amplitude is too strong. Simulated Northern Hemisphere extratropical wintertime atmospheric circulation, especially the NAO pattern, and its variability are quite well reproduced by the model [Min *et al.*, 2005b].

[5] The main forcings driving the model, CO_2 , CH_4 , solar variations and effective volcanic forcing are described in detail by Zorita *et al.* [2005]. For this analysis, the volcanic forcing is implemented as a reduction of the solar constant. Yoshimori *et al.* [2005] also implemented this forcing in the CSM model and found a NAO response and high-latitude winter warming after “volcanic eruptions.” The mechanism does not involve stratospheric aerosols but just tropospheric temperature gradient.

[6] Simulated monthly anomalies, relative to the long-term 1000–1990 mean, have been filtered using a recursive Butterworth filter with a cut-off at 0.1 cycle-per-year to remove the long-term variability, which could blur the typical ENSO-related variability. Several regional indices have been computed; Niño3 index is defined as the average of the SSTA between $[150\text{W}–90\text{W}$ and $5\text{S}–5\text{N}]$ [Min *et al.*, 2005a, 2005b] and warm (207 events) and cold (199 events) ENSO are defined as Niño3 anomalies $> 1\text{C}$ and $< -1\text{C}$, respectively. A Tropical Atlantic SSTA index (TROP_ATL) is the average of the SSTA in the region $[60\text{W}–0$ and $0–25\text{N}]$. A North Atlantic SLPA index (NATL) is defined as the difference between the average of SLPA in the region $[10\text{W}–60\text{W}$ and $30\text{N}–45\text{N}]$ and in the region $[10\text{W}–70\text{W}$ and $50\text{N}–70\text{N}]$ and corresponds roughly to the NAO. An Aleutian SLPA index (AL) is the

average of the SLPA in $[160\text{W}–130\text{W}$ and $40\text{N}–60\text{N}]$, that is the mean location of the Aleutian low.

3. Results

3.1. Mean SLPA Response

[7] Following Moron and Gouirand [2003], composite mean SLPA associated to warm and cold ENSO events have been calculated for the 1000–1990 period in November–December and January–March (Figure 1) and on ten 100-years sub-periods (1001–1100, 1101–1200, ... 1901–1990 (not shown)). In November–December, there is a significant strengthening (weakening) of the Aleutian low during the warm (cold) ENSO events (Figures 1a and 1b). Over the North-Atlantic, the ENSO response is weak (Figures 1a and 1b). In January–March, the deepening (weakening) of the Aleutian low during the warm (cold) ENSO events is stronger than in November–December, which also happens for the positive (negative) SLPA over the north-central and north-eastern parts of North America (Figures 1c and 1d). Over North Atlantic, the SLPA during the warm ENSO events is now close to the negative (positive) NAO-like pattern (i.e. positive (negative) SLPA north (south) of 45N) and vice-versa for the cold ENSO events (Figures 1c and 1d). SLPA associated with cold ENSO events are slightly stronger (Figures 1c and 1d). The hypothesis of the stationarity of the relationship between NATL and ENSO in January–March is tested using a bootstrap method. The standard deviation of averaged NATL anomalies corresponding to warm and cold ENSO events during running 50- and 100-year periods is computed. The significance level is assessed with the standard deviations, computed in the same way, from randomly permuted pairs of NATL and Niño3 time series. The model standard deviations are always surpassed by at least 25% of the bootstrapped ones. The null hypothesis that the relationship between NAO and Niño3 is stationary at multi-decadal

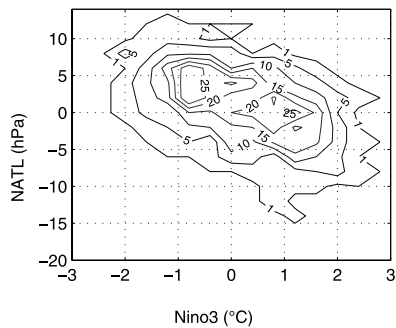


Figure 2. Contour plot between high-pass filtered (i.e. without frequencies < 0.1 cycle-per-year) Niño3 (in C) in abscissa and NATL (in hPa) in ordinates. The frequency is counted by bins of 2 hPa and 0.4C and the contours are drawn for 1, 5, 10, 15, 20 and 25 observations in bin.

time scales in this ECHO-G simulation cannot be rejected, consistent with the findings of Brönnimann *et al.* [2007] using climate reconstructions. Moreover, there is no systematic increase of the NATL anomalies at the end of the simulation (not shown). In summary, the ECHO-G model is able to reproduce a realistic and stationary mean North America/North-Atlantic response to the ENSO events in January–March [Moron and Gouirand, 2003]. The simulated atmospheric response over the North Atlantic in November–December is weak and not consistent with the one observed during the contemporaneous period [Moron and Gouirand, 2003].

[8] The relation between Niño3 and NATL is globally linear and stronger than for the contemporaneous period (Figure 2; $r = -0.49$). However, if we focus separately on warm and cold ENSO events ($r = -0.12$ and -0.13 for NATL-Niño3 correlations on warm and cold ENSO events), it appears that the intensity of the equatorial Pacific SST seems not to be the main factor for the strength and polarity of the North-Atlantic SLPA response. In other words, it means that when analyzing warm and cold ENSO events separately, the bulk of ENSO signal is almost filtered out, leaving a large inter-event variability (not related to ENSO), also suggested by the dispersion around the mean linear response (Figure 2).

3.2. Inter-Event Variability

[9] We now focus on the inter-event variability of North Atlantic SLPA in January–March only. The SLPA pattern in phase with the mean composites (Figures 1c and 1d) will be called hereafter ‘typical’ response (i.e. negative (positive) NATL for warm (cold) events) and the SLPA out of phase with the mean composites (Figures 1c and 1d) will be called ‘non typical’ response (i.e. positive (negative) NATL for warm (cold) events). According to Robock [2000], the tropical volcanic eruptions are associated with a positive NAO phase in the following few winters. In that sense, in the real world, the ‘non typical’ (respectively ‘typical’) response to warm (respectively cold) ENSO events should be more prevalent following volcanic eruptions. The Robock response is mostly due to the stratospheric aerosols and the meridional gradient of the heating (i.e. more heating in the tropics than in high latitudes). The volcanic forcing is

here spatially uniform and the NATL response to volcanism doesn’t include Robock’s mechanism, so that, in principle, we cannot expect a classical Robock response in the model. Indeed, 25 out of 158 (9/49) warm ENSO events are associated with a ‘typical’ (‘non typical’) SLPA response and a volcanic eruption in the simulation. Both ratios are not significantly different suggesting that volcanic eruptions, introduced here as a simple decrease of the solar constant, do not systematically induce a non typical response during warm ENSO events in the model. Similarly 30/160 (8/39) cold ENSO events are associated with a ‘typical’ (‘non typical’) response and a volcanic eruption. The occurrence of a ‘typical’ response during cold ENSO events associated with a volcanic eruption is thus not stronger. This is also observed when the eruptions occurring one and two years before the ENSO events are included (not shown).

[10] To test the influence of atmospheric and oceanic forcings on the SLPA response over the North Atlantic, four samples have been extracted: (1) warm and (2) cold ENSO events associated with the ‘typical’ SLPA response over the North Atlantic (i.e. respectively Niño3 > 1 C and NATL < 0 and Niño3 < -1 C and NATL > 0), and (3) warm and (4) cold ENSO events associated with ‘non typical’ SLPA response over the North Atlantic (i.e. respectively Niño3 > 1 C and NATL > 0 and Niño3 < -1 C and NATL < 0). Subequatorial SSTA (5N–5S) have been firstly averaged across the Pacific and the location in longitude and intensity of SSTA have been extracted for each warm and cold ENSO events. The occurrence of ‘typical’ versus ‘non typical’ ENSO is not related to a significantly different location in longitude and/or intensity of the warm or cold SSTA in the subequatorial Pacific (not shown). The sensitivity of the North Atlantic atmosphere anomalies to a “dateline” or “conventional” (i.e. Eastern Pacific) location of the highest SSTA depicted by Larkin and Harrison [2005] in reanalyses is thus not found in this simulation. Then, the monthly mean of SLP and SST indices has been computed from November to March (Figure 3). Note that the largest North Atlantic SLPA (i.e. dashed line in Figure 3a) are observed in February as in the observations [Moron and Gouirand, 2003]. As suggested before, the intensity of Niño3 anomalies (full line in Figures 3c and 3d) are not significantly different between the ‘typical’ and ‘non typical’ warm (and cold) ENSO events. TROP_ATL anomalies are significantly different between the ‘typical’ and ‘non typical’ warm and cold ENSO events in February and March (dash-dotted bold line in Figures 3c and 3d), but this SSTA difference could be forced by the different SLPA pattern. AL anomalies exhibit rather large differences in January and February (grey bold lines in Figures 3a and 3b, Table 1). A possibly unstable atmospheric see-saw between Aleutian and Icelandic low [Honda *et al.*, 2001] could be then a significant factor of modulation of the ENSO teleconnection over the North Atlantic domain.

4. Conclusion

[11] The aim of this paper was to analyze the North Atlantic SLPA response to warm and cold ENSO events and to test the possible origins of its inter-event variability in a quasi-millennial (1000–1990) run of ECHO-G model. Such analysis is needed in the context of long-term climate

changes as those associated with the increase of greenhouse gases [Müller and Roeckner, 2006]. SLPA and SSTA have been high-pass filtered to focus on the typical timescale of ENSO (i.e. less than 10 years). In November–December, the North Atlantic response is weak and not in agreement with the observations [Moron and Gouirand, 2003]. The mean SLPA are stronger and quite realistic in January–March. In this season, the mean SLPA associated to warm (cold) events simulated by ECHO-G model correspond to a strengthening (weakening) of the Aleutian low, positive (negative) SLPA over the north-central and north-eastern parts of North America, and to a negative (positive) NAO-like pattern over the North Atlantic area. The North Pacific/North America response is already observed in November–December but with a weaker amplitude. This SLPA pattern in January–March is similar to the one observed by Pozo-Vazquez et al. [2001] and Gouirand and Moron [2003] for the contemporaneous period and by Brönnimann et al. [2007] for the last three centuries. The relationship between ENSO and North Atlantic SLPA is stationary at multi-decadal time scales, and in particular, does not increase at the end of the 20th century. The linear relationship between North Atlantic SLPA and ENSO is stronger than in observed record, partly because model filters out some of the atmospheric noise and also because the timescale of modelled ENSO is shorter than in observations, and thus closer to the interannual variability of the NAO.

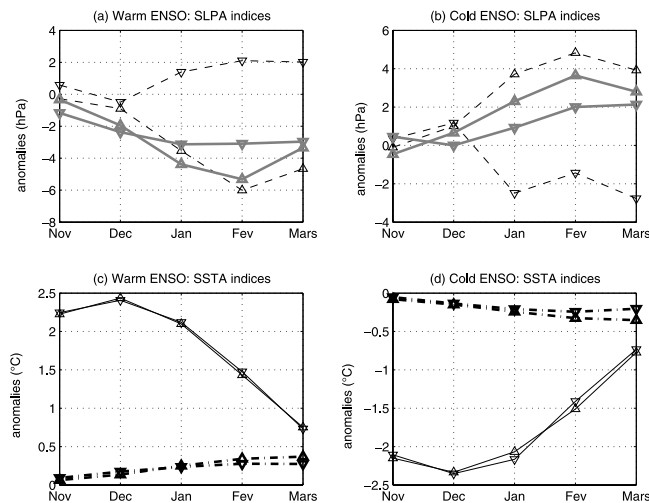


Figure 3. Monthly mean anomaly of (a, b) sea level pressure indices (NATL index, dashed line; AL index, grey full line), and (c, d) sea surface temperature indices (Niño3 index, full line; TROP_ATL index, dash-dotted bold line) during warm (Figures 3a and 3c) and cold (Figures 3b and 3d) El Niño Southern Oscillation (ENSO) events for the ‘typical’ (triangle-up) and the ‘non typical’ (triangle-down) samples. Warm and cold ENSO are determined as high-pass filtered (i.e. without frequencies < 0.1 cycle-per-year) Niño3 sea surface temperature anomalies $> 1\text{C}$ and $< -1\text{C}$ respectively. The ‘typical’ and ‘non typical’ samples correspond respectively to positive (negative) and negative (positive) North Atlantic Oscillation phase (determined from the NATL index) in January–March during cold (warm) ENSO events.

Table 1. p-Value of Student’s T Test of the Difference Between ‘Typical’ and ‘Non Typical’ Warm and Cold El Niño Southern Oscillation Events for Aleutian Sea Level Pressure Index Between November and March^a

	November	December	January	February	March
Cold ENSO	0.21	0.47	0.09	0.07	0.40
Warm ENSO	0.22	0.60	0.11	<0.01	0.58

^aAleutian sea level pressure index is the average of sea level pressure anomalies in 160–130W and 40–60N. The warm and cold ENSO events are defined as Niño3 sea surface temperature anomalies $> 1\text{C}$ and $< -1\text{C}$ respectively using high-pass filtered data (without frequencies < 0.1 cycle-per-year). The ‘typical’ and ‘non typical’ samples correspond respectively to positive (negative) and negative (positive) North Atlantic Oscillation phase (from the North Atlantic sea level pressure index) in January–March during cold (warm) ENSO events.

[12] The model also shows inter-event variability in the ENSO-related response, in agreement with observations and climate reconstructions [Pozo-Vazquez et al., 2001; Gouirand and Moron, 2003; Brönnimann et al., 2007]. This inter-event variability seems neither associated with the intensity and the location in longitude of the warm or cold ENSO events, nor with the intensity of Tropical Atlantic SSTA, at least at high frequency, also in agreement with previous observational studies [Moron and Gouirand, 2003; Pozo-Vazquez et al., 2005]. It seems that the effective volcanic forcing implemented in the model as a simple decrease of the solar constant is not able to systematically modulate the North Atlantic SLPA response to ENSO, but it could be related to the lack of realism in producing a meridional thermal gradient in the stratosphere. The results also show that the magnitude of SLPA over the North Pacific is weaker in January–February when the SLPA pattern over North Atlantic is out-of-phase with the mean response. There are no precursors in North Pacific SLPA and it is difficult to conclude if both sectors interact through internal atmospheric dynamics as Rossby wave, or are both forced by another factor not considered here.

References

- Brönnimann, S., E. Xoplaki, C. Casty, A. Pauling, and J. Luterbacher (2007), ENSO influence on Europe during the last centuries, *Clim. Dyn.*, **28**, 181–197, doi:10.1007/s00382-006-0175-z.
- Cassou, C., and L. Terray (2001), Oceanic forcing of the wintertime low frequency atmospheric variability in the North-Atlantic European sector: A study of the ARPEGE model, *J. Clim.*, **14**, 4266–4291.
- Gouirand, I., and V. Moron (2003), Variability of the impact of El Niño–Southern Oscillation on sea-level pressure anomalies over the North Atlantic in January to March (1874–1996), *Int. J. Climatol.*, **23**, 1549–1566.
- Honda, M., H. Nakamura, J. Ukita, and K. Takeuchi (2001), Interannual seesaw between the Aleutian and the Icelandic lows. part II: Its significance in the interannual variability over the wintertime Northern Hemisphere, *J. Clim.*, **14**, 1029–1042.
- Huang, J., K. Higuchi, and K. L. Shabbar (1998), The relationships between the North Atlantic Oscillation and El Niño Southern Oscillation, *Geophys. Res. Lett.*, **25**, 2707–2710.
- Kumar, A., and M. P. Hoerling (1998), Annual cycle of the Pacific–North American seasonal predictability associated with different phases of ENSO, *J. Clim.*, **11**, 3295–3308.
- Larkin, N. K., and D. E. Harrison (2005), Global seasonal temperature and precipitation anomalies during El Niño autumn and winter, *Geophys. Res. Lett.*, **32**, L16705, doi:10.1029/2005GL022860.
- Lee, E. J., J. G. Jhun, and J. G. Kang (2002), The characteristic variability of boreal wintertime atmospheric circulation in El Niño events, *J. Clim.*, **15**, 892–904.
- Legutke, S., and R. Voss (1999), The Hamburg atmosphere–ocean coupled circulation model ECHO-G, *Tech. Rep. 18*, 62 pp., Dtsch. Klimarechenzentrum, Hamburg, Germany.

- May, W., and L. Bengtsson (1998), The signature of ENSO in the Northern Hemisphere midlatitude seasonal mean flow and high-frequency intraseasonal variability, *Meteorol. Atmos. Phys.*, *69*, 81–100.
- Min, S. K., S. Legutke, A. Hense, and W. T. Kwon (2005a), Internal variability in a 1000-yr control simulation with the coupled climate model ECHO-G. I: Near-surface temperature, precipitation and mean sea level pressure, *Tellus, Ser. A*, *57*, 605–621.
- Min, S. K., S. Legutke, A. Hense, and W. T. Kwon (2005b), Internal variability in a 1000-yr control simulation with the coupled climate model ECHO-G. II: El Niño Southern Oscillation and North Atlantic Oscillation, *Tellus, Ser. A*, *57*, 622–640.
- Mo, K. C., and R. E. Livezey (1986), Tropical-extratropical geopotential height teleconnections during the Northern Hemisphere winter, *Mon. Weather Rev.*, *114*, 2488–2515.
- Moron, V., and I. Gouirand (2003), Seasonal modulation of the ENSO relationships with sea level pressure anomalies over the North Atlantic in October–March 1873–1996, *Int. J. Climatol.*, *23*, 143–155.
- Moron, V., and G. Plaut (2003), The impact of the ENSO on weather regimes over North-Atlantic and Europe during boreal winter, *Int. J. Climatol.*, *23*, 363–379.
- Müller, W. A., and E. Roeckner (2006), ENSO impact on midlatitude circulation patterns in future climate change projections, *Geophys. Res. Lett.*, *33*, L05711, doi:10.1029/2005GL025032.
- Pozo-Vazquez, D., M. J. Esteban-Parra, F. S. Rodrigo, and Y. Castro-Diez (2001), The association between ENSO and winter atmospheric circulation and temperature in the North Atlantic region, *J. Clim.*, *14*, 3408–3420.
- Pozo-Vazquez, D., S. R. Gamiz-Fortis, J. Tovar-Pescador, M. J. Esteban-Parra, and Y. Castro-Diez (2005), El Niño Southern Oscillation events and associated European winter precipitation anomalies, *Int. J. Climatol.*, *25*, 17–31.
- Robertson, A. W., C. R. Mechoso, and Y. J. Kim (2000), The influence of the Atlantic sea surface temperature anomalies on the North Atlantic Oscillation, *J. Clim.*, *13*, 122–138.
- Robock, A. (2000), Volcanic eruptions and climate, *Rev. Geophys.*, *38*, 191–219.
- Roeckner, E., K. Arpe, L. Bengtsson, M. Christoph, M. Clausen, L. Dümenil, M. Esch, M. Giorgetta, U. Schlese, and U. Schulzweida (1996), The atmospheric general circulation model ECHAM4: Model description and simulation of present-day climate, *Rep. 218*, 90 pp., Max Planck Inst. für Meteorol., Hamburg, Germany.
- Ropelewski, C. F., and M. S. Halpert (1987), Global and regional precipitation patterns associated with the ENSO, *Mon. Weather Rev.*, *115*, 1606–1626.
- Wallace, J. M., and D. S. Gutzler (1981), Teleconnections in the geopotential height field during the Northern Hemisphere winter, *Mon. Weather Rev.*, *109*, 784–812.
- Wolff, J. O., E. Maier-Reimer, and S. Legutke (1997), The Hamburg ocean primitive equation model, *Tech. Rep. 13*, 98 pp., Dtsch. Klimarechenzentrum, Hamburg, Germany.
- Yoshimori, M., T. F. Stocker, C. Raible, and M. Renold (2005), Externally forced and internal variability in ensemble climate simulations of the Maunder Minimum, *J. Clim.*, *18*, 4253–4270.
- Zorita, E., J. F. González-Ruoco, H. von Storch, J. P. Montávez, and F. Valero (2005), Natural and anthropogenic modes of surface temperature variations in the last thousand years, *Geophys. Res. Lett.*, *32*, L08707, doi:10.1029/2004GL021563.

I. Gouirand and V. Moron, CEREGE, Europôle Méditerranéen de l'Arbois, BP 80, F-13545 Aix en Provence, France. (gouirand@hotmail.com)

E. Zorita, Institute for Coastal Research, Building 38, Room 314, Max-Planck-Strasse 1, D-21502 Geesthacht, Germany.